

## Classical microscopic calculations of high-energy collisions of heavy ions\*

A. R. Bodmer and C. N. Panos

Argonne National Laboratory, Argonne, Illinois 60439  
and University of Illinois at Chicago Circle, Chicago, Illinois 60680

(Received 30 August 1976)

Nonrelativistic classical microscopic (equations of motion) calculations have been made for collisions between nuclei mostly with 50 nucleons each and for relative velocities of  $0.5c$  and  $0.8c$  (nonrelativistic laboratory energies of 117 and 300 MeV/nucleon, respectively). The trajectories of all the nucleons are calculated with two-body forces between all pairs of nucleons. The potentials are sums of attractive and repulsive Yukawa potentials of reasonable ranges and are adjusted to give reasonable binding and kinetic energies and to fit the  $NN$  cross section  $\sigma_v$  appropriate for the viscosity and thus for shock phenomena;  $\sigma_v$  strongly emphasizes transverse momentum transfers. Ensemble averages are taken over (10) initial distributions and care is taken to monitor—the relatively minor—effects of evaporation of the individual noninteracting nuclei. Central collisions corresponding to small impact parameters  $b$  (less than about a nuclear radius  $R$ ) are “explosive” and seem fairly well equilibrated at maximum compression and subsequently. There is some similarity to development of shocks. After an initial penetration of about a mean free path, there is rapid dissipation of the collisional translational energy with associated large internal energies and large compressions (to somewhat less than twice normal density), followed finally by an explosive expansion; the angular distributions are roughly isotropic for quite small  $b$  but show some transverse peaking for very small  $b$ . For small  $b$  ( $\lesssim 0.5R$ ) and for  $v = 0.5c$ , but not for  $0.8c$ , we find large fused residues with  $A \approx 60$ . Transparency and nonequilibrium effects develop rapidly with increasing  $b$  and are somewhat more important for  $v = 0.8c$  than for  $0.5c$ . For  $b \gtrsim R$  (noncentral collisions) the nuclei retain much and for  $b \gtrsim 1.5R$  most of their initial identity, suffering relatively little immediate mass loss with, however, quite appreciable loss of collisional translational energy for  $b \approx R$ .

[NUCLEAR REACTIONS HI classical nonrelativistic microscopic calculations;  
mostly  $A_1=A_2=50$ ;  $E=117, 300$  MeV/nucleon.]

### I. INTRODUCTION

#### A. Hydrodynamics and nuclear shock waves

The only apparent means of experimentally producing nuclear matter at densities significantly greater than the normal density  $\rho_0$  ( $\approx 0.2$  nucleons  $\text{fm}^{-3}$ ) of nuclear matter seems to be in heavy-ion collisions at laboratory energies  $E_L \gtrsim 50$  MeV/nucleon. At such energies the relative velocities of the nuclei are greater than the sound velocity  $c_s \approx 0.2c$  in normal nuclear matter or, roughly equivalent, greater than the Fermi velocity  $v_F \approx 0.3c$  ( $c$  is the velocity of light). Compressible hydrodynamics, mostly used with the assumption of zero viscosity (inviscid hydrodynamics), then implies shock-wave phenomena associated with characteristic Mach-cone features of the angular distributions which may then be rather directly related to the equation of state.<sup>1-9</sup> Thus, e.g., for “weak” shocks<sup>1</sup> (equivalent to sound waves), for which the changes in the physical quantities across the shock are small, the Mach cone would determine  $c_s$  and thus the “compressibility” coefficient  $K$  of nuclear matter at  $\rho_0$ , since  $c_s^2 = K/9M$ , where  $M$  is the nucleon mass. ( $K$  is about 200 MeV.)

For relative velocities considerably larger than  $c_s$  one has the possibility of “strong” shocks, involving large compressions, and hence of obtaining knowledge of the equation of state at densities much greater than  $\rho_0$ .<sup>2-9</sup> Thus, e.g., if there should be density isomers<sup>10,11</sup> corresponding to a second minimum in the equation of state at  $\rho > \rho_0$ , then this might reflect itself in the angular distributions and, in particular, in their energy dependence.<sup>9,12</sup>

For orientation we note that, nonrelativistically, for an ideal gas, the maximum possible compression across a shock is  $(\rho/\rho_0)_{\max} = (\gamma + 1)/(\gamma - 1)$  where  $\rho_0$  and  $\rho$  are the densities in front of and behind the shock, respectively, and where  $\gamma$  is the usual ratio of specific heats.<sup>13</sup> Thus  $(\rho/\rho_0)_{\max} = 4, 6,$  and  $8,$  respectively, for an ideal monoatomic gas ( $\gamma = \frac{5}{3}$ ), for a gas of diatomic molecules with only rotational degrees of freedom ( $\gamma = \frac{7}{5}$ ), and for diatomic molecules with both vibrational and rotational degrees of freedom ( $\gamma = \frac{9}{7}$ ). We recall that if the nuclei are free to pass through each other without mutual interaction then  $\rho_{\max} = 2\rho_0$ . However, densities less than  $2\rho_0$  may also correspond to hot thermalized nuclear matter.

### B. Validity of hydrodynamics

Hydrodynamics as considered in Refs. 1–9 for high-energy heavy-ion collisions is the usual hydrodynamics as used for normal macroscopic fluids. Its validity seems to depend on two assumptions.

(1) The validity of classical considerations. These are expected to become more reasonable at high energies ( $E \gg E_F$ ) when, e.g., the effects of the Pauli principle and of exchange effects become much reduced. However, it should be noted that hydrodynamics, although “essentially” classical, can include important quantum-mechanical effects through the equation of state.

(2) The continuum assumption. This requires that local thermodynamic equilibrium be attained in times short compared to the collision time, i.e., that  $\chi \equiv \tau_{\text{rel}}/\tau_{\text{col}} \ll 1$ . Here  $\tau_{\text{col}} = L/v$  is a typical collision time,  $L$  is a characteristic collision length, and  $v$  is a typical relative nucleon-nucleon velocity;  $\tau_{\text{rel}} = \Lambda/v_{\text{rel}}$  is a typical relaxation time where  $\Lambda$  is the mean-free path and  $v_{\text{rel}}$  is about  $c_s$  or  $v_F$  (possibly better about  $v$  for  $v > v_F$ ). In any case, for  $v = O(v_{\text{rel}})$  the condition  $\chi \ll 1$  is then essentially equivalent to  $\Lambda \ll L$ , i.e., to a short mean free path.<sup>6,14</sup>

The relevant length scales are as follows:  $\Lambda \approx 2$  fm (appropriate to laboratory energies of a few hundred MeV/nucleon),  $L \approx 2$ –3 fm for “peripheral” or equivalently noncentral collisions corresponding (for equal mass nuclei) to impact parameters  $b \gtrsim R$  where  $R$  is the nuclear radius ( $L$  corresponds to about the average overlap distance obtained in Ref. 15 for fragmentation collisions), and  $L \approx R \approx 5$  fm for central collisions. For subsequent considerations we also introduce the force range  $d \approx 1$  fm. With  $v/c \approx 0.5$ –0.8, the corresponding time scales are then  $\tau_{\text{rel}} \approx 7$  fm/ $c$  (with  $v_{\text{rel}} \approx v_F$ ),  $\tau_{\text{col}}(\text{peripheral}) \approx 3$  fm/ $c$ ,  $\tau_{\text{col}}(\text{central}) \approx 8$  fm/ $c$  and  $\tau_{NN} = d/v \approx 2$  fm/ $c$  for the duration of an individual  $NN$  collision.

Thus  $\chi \approx 2$  for peripheral collisions and  $\chi \approx 1$  for central collisions. The continuum assumption is thus at best marginally satisfied for central collisions of heavier nuclei while peripheral collisions especially can be expected to have marked non-equilibrium features.

We note that a shock would not be instantaneously formed on contact of the two nuclei but would need distances of the order of  $\Lambda$  to be established via dissipative processes, i.e., through collisional relaxation. Furthermore, a shock is not a discontinuity in a complete microscopic description, or according to viscous hydrodynamics, but has structure and in particular a thickness of the order of  $\Lambda$ .<sup>13</sup> Since  $\Lambda$  is not negligible compared with

$R$ , such effects could by themselves significantly modify the shock-wave predictions of inviscid hydrodynamics.<sup>16</sup>

If the continuum assumption is not satisfied, questions such as the following immediately arise. How are the predictions of hydrodynamics modified by the relaxational effects of the collisions, i.e., by mean-free path effects? In particular, what is the importance of dissipative effects (viscosity, thermal conduction, etc.) and of transparency? For what conditions may one expect approximate thermal equilibrium, shock-type phenomena, and associated high densities? What are the characteristics of the corresponding collisions? What can one learn about the equation of state or about transport coefficients?

### C. Classical microscopic (equations-of-motion) approach

To avoid the limitations of hydrodynamics and to attempt to answer some of the above questions we have made classical nonrelativistic equations-of-motion (EOM) calculations where all the nucleon trajectories are computed with suitable two-body forces between all pairs of nucleons.<sup>17–19</sup> Meson production is not included and the nucleons are taken to be spinless.

The following are some aspects—and, in particular, advantages—of a classical microscopic EOM approach, including its relation with other, also essentially classical descriptions (see Fig. 1). These descriptions include, in particular, hydrodynamics, discussed above, and a microscopic approach using the Boltzmann equation or equivalently cascade calculations.<sup>20</sup>

(1) Classical considerations may be expected to be reasonably good for laboratory energies  $E_L \gtrsim 250$  MeV/nucleon and qualitatively reasonable for  $E_L \gtrsim 100$  MeV/nucleon. Thus the nucleon wavelengths ( $\lesssim 1$  fm) are then comparable or smaller than the force range  $d$  or the mean interparticle distance; the classical and quantum mechanical results for the cross section  $\sigma_v$ , appropriate for transverse momentum transfer (Sec. IID) become quite close to each other for  $E_L \gtrsim 250$  MeV; degeneracy effects expected to be of order  $E_F/E_L$  are expected to become quite small. Also, classical approximations are expected to be better as a result of averaging over final states (generally no definite final states are observed and the reactions are of the inclusive type, e.g., as in Ref. 15).

(2) The classical  $N$ -body problem is computationally feasible for quite large  $N$ .<sup>21</sup>

(3) All  $3A$  translational degrees of freedom of the nucleons are included. Thus, e.g., collective

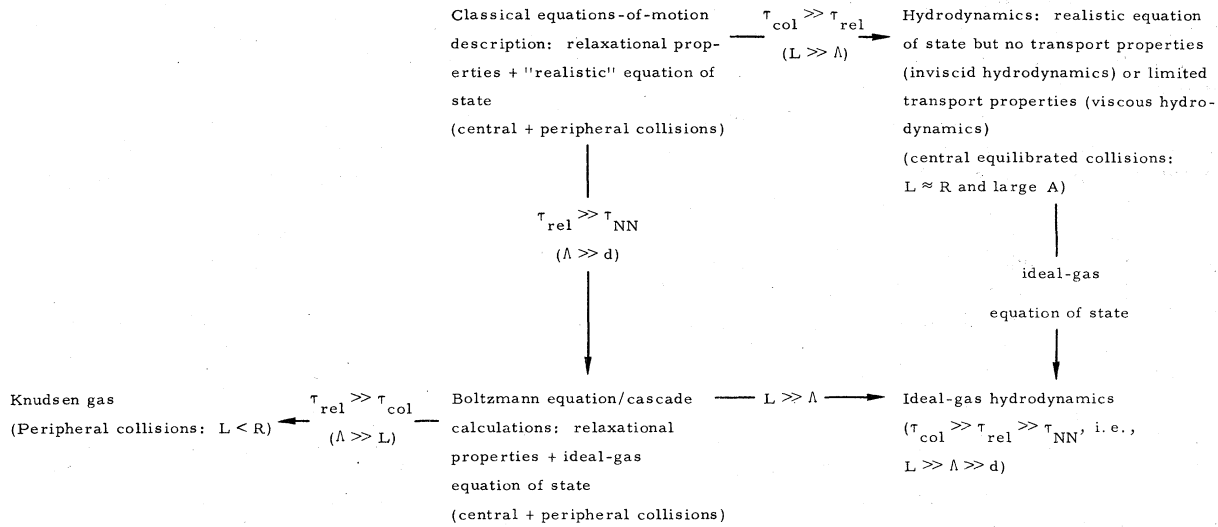


FIG. 1. Classical descriptions of high-energy heavy-ion collisions. See Sec. IC for discussion.

effects, insofar as they are important at high energies, are included. Binding-energy effects, including surface effects, are allowed for; in particular, the possibility of final bound fragments is included.

(4) Equilibrium, near equilibrium, or partial equilibrium is not assumed and the relaxational effects of elastic  $NN$  collisions are included. Thus highly nonequilibrium situations can be described and all dissipative and transport phenomena due to elastic  $NN$  collisions are included.

(5) The use of the Boltzmann equation or equivalently of cascade calculations<sup>20</sup> is included as a limit when  $\Lambda \gg d$  or equivalently  $\tau_{NN} \ll \Lambda/v$ , i.e., if the duration of individual  $NN$  collisions is short compared to the time between collisions. Correspondingly, there is no overlapping between successive collisions involving a given nucleon and one has straight-line undeflected trajectories between collisions. This limit then implies a dilute gas with the ideal-gas equation of state. The Boltzmann-equation and cascade approaches make direct use of the  $NN$  differential cross sections (in the Boltzmann equation these enter through the collision term) and thus implicitly include quantum mechanical aspects of the individual  $NN$  scattering process, but otherwise they are classical. These microscopic approaches can also describe arbitrarily large deviations from equilibrium, such as shock waves (but only if the full nonlinear collision term is used in the Boltzmann equation or if in cascade calculations the cascade is completely followed in time).<sup>22</sup> However, because of the implied ideal-gas equation of state, the shock relations—and in particular

the maximum compressions—will be those appropriate to an ideal gas. However, some account can be taken of forces in cascade-type calculations as in Ref. 19 where hard-sphere  $NN$  scattering is considered; such calculations are then intermediate in nature between EOM and cascade calculations. It is clear that the condition  $\Lambda \gg d$  is not well satisfied in high-energy heavy-ion collisions. (6) Inviscid as well as viscous hydrodynamics is contained in the EOM approach in the limit of local, or approximately local, thermodynamic equilibrium, i.e.,  $\tau_{rel} \ll \tau_{col}$  (or  $\Lambda \ll L$ ).<sup>23,24</sup> At the other extreme, when  $\Lambda \gg L$ , the case of large transparency (a Knudsen gas) is also included. High-energy heavy-ion collisions may have aspects characteristic of both these limits. Thus noncentral (peripheral) collisions for which  $L < R$  ( $L \approx 2$  fm), correspond to large transparency and strong nonequilibrium conditions, whereas sufficiently central collisions ( $L \approx R$ ) may be fairly well equilibrated (especially for heavier nuclei) and correspond perhaps more closely to a hydrodynamic regime. A microscopic approach thus seems to be needed for a unified description of heavy-ion collisions.

#### D. Twofold role of nuclear forces

For high-energy heavy-ion collisions one may then conveniently distinguish two roles for the forces.

1. For determining the equation of state. This in turn determines the relation between the physical quantities before and behind a shock. This aspect of the forces is the only one which enters

into (inviscid) hydrodynamics and which gives the hydrodynamic predictions their relative simplicity. In particular, we note that "strong" shocks, involving large increases of density, are probably only possible because nuclear matter is rather dilute with respect to the repulsive core and thus rather readily compressible.

2. For determining the collisional relaxation effects. These are the mean-free path and dissipative effects which are completely neglected in inviscid hydrodynamics. It is these aspects of the forces which are essential for the formation of the shock and for shock structure. Their importance is characterized by the ratio  $\tau_{\text{rel}}/\tau_{\text{col}}$ .<sup>25</sup>

The EOM approach is the only classical description which can take account of both roles of the forces. If nuclear matter were very dilute, and thus approximately an ideal gas, then the primary role of the forces would be their relaxational one. The Boltzmann equation or cascade calculations would then be expected to provide an adequate description.

## II. CALCULATIONAL PROCEDURES AND NUCLEAR FORCES

### A. Trajectory computations

For two nuclei with  $A_1$  and  $A_2$  nucleons the  $A = A_1 + A_2$  trajectories corresponding to a set of initial conditions are obtained by integrating Newton's equations of motion with use of two-body potentials and the corresponding forces between all pairs of nucleons. Conservation of momentum, angular momentum, and energy are checked. The first two, being linear in the momenta, are very accurately conserved. A time (integration) interval of 0.1 fm/c was found to mostly give adequate energy conservation (to about 1%) and reasonable computing times.<sup>21</sup>

### B. Initial conditions, averaging

For given collision conditions, specified by  $A_1$ ,  $A_2$ , impact parameter  $b$ , and laboratory energy  $E_L$ , one must (ensemble) average over initial distributions of positions and velocities in each nucleus. The impact parameter  $b$  was varied from 0 to  $2R$  in steps of  $0.25R$  with the nuclei initially almost touching.

Our distributions of positions correspond to nuclei of radius  $R = r_0 A_i^{1/3}$  with  $r_0 \approx 1.15$  fm. With repulsive-core potentials (see below), random distributions of positions inside a sphere of radius  $R$  are generally very hot, i.e., energetically very unfavorable, since, in particular, nucleons may be sufficiently close to each other for the short-range repulsion to be very large.

The individual nuclei which are used for the initial distributions in the collision calculations have then been prepared in three stages as follows.

1. A random distribution of ( $A_i$ ) particle positions is generated in a sphere of radius  $R$ .

2. With the initial particle velocities equal to zero, this distribution (which is very hot) is allowed to dynamically evolve with use of repulsive-core potentials. However, the particle velocities are reset to zero at predetermined time instants (the corresponding time intervals are very short during the early very hot stages); thus the initial velocities are zero for the succeeding interval of the evolution. Various quantities (see also Sec. IIC) are monitored, in particular the density  $\rho$ , various moments of  $\rho$ , the potential energy/nucleon  $V$ , and the kinetic energy/nucleon. After  $V$  has decreased from its initial very large value and has settled down and is very slowly varying, and also before the density distribution has changed very much from its initial value, the corresponding particle positions are used as the *initial positions* for the initial nuclei used in the collision calculations. The result of this stage is to dynamically cool the initial random position distributions without allowing too much change in  $\rho$  although these distributions do have somewhat too large densities.

3. The velocities for the distributions obtained in stage 2 are reset such that the particle velocities correspond to random velocity distributions appropriate to a Fermi sphere with an average kinetic energy of about 22–25 MeV/nucleon. Minor adjustments are made to the kinetic energy such that for the potentials used in the collision calculations the average binding energy/nucleon is 8 MeV for each distribution; the average potential energy/nucleon for the ensemble is then about 30 MeV.<sup>26</sup>

These classical nuclei have a finite temperature not only because of the kinetic energy (which plays an important role as discussed especially in Sec. IIIF) but also because (with the kinetic energy equal to zero) the potentials give a minimum energy (as a function of  $\rho$ ) at densities considerably larger than  $\rho_0$ . (Such a minimum with the nucleons at rest corresponds to "frozen" nuclei of zero temperature for which the nucleons are arranged approximately in a lattice.) Nevertheless, our nuclei are probably as cold as possible, consistent with a reasonable density, kinetic energy, and binding energy for static repulsive-core potentials with the required scattering properties (see below) and, furthermore, with pair distributions which do not correspond to "frozen" nuclei but are appropriate to the nucleons being allowed

to move freely consistent with the dynamics.

The nuclei are thus not stationary and simultaneously condense and evaporate. However, the time scale for these changes is sufficiently long, relative to the collision time, that the mutual interactions of the nuclei dominate during the collision. (To minimize the effect of changes due to evaporation, the nuclei are initially almost touching.) Nevertheless, for any set of collision conditions, it is important to obtain as a standard of reference and for purposes of normalization the results without *mutual* interaction, i.e., when only the interactions in *each nucleus separately* are operative.<sup>27</sup> Some further considerations and relevant results are given below (especially Sec. III A).

Our most extensive results are for  $A_1 = A_2 = 50$  where we used an ensemble of 10 different initial distributions.<sup>28</sup> Because  $A$  is rather large there is effectively considerable averaging even for each initial distribution.

In fact, our results for averages involving a reasonable number of particles are fairly smooth and well-behaved functions of the time or of any relevant spatial coordinate. Of course, the variations are larger for averages of "more local" quantities, e.g., populations and the corresponding densities for volume elements containing only a few particles.

The physical quantities will not be unique at each instant but have some distribution with a corresponding dispersion about the mean. One must be careful not to miss interesting information such as clustering by looking only at the averages where such information may be largely lost.

### C. Analysis

The  $A$  trajectories are analyzed to give kinetic and potential energies, populations, position and velocity moments, hydrodynamic-type averages such as densities, average (collective) velocities, etc., as well as some quantities (especially pertaining to angular distributions) involving both the position and velocity distributions, all as a function of time. Analyses were made, in the center of mass (c.m.) system, both in cylindrical polar coordinates and in spherical polar coordinates with the incident direction as polar axis.<sup>29</sup> The former is especially appropriate for the earlier stages of collisions with small or moderate impact parameters, while the latter is more appropriate for the later stages and, in particular, for the angular distributions. The latter are obtained from the distribution of particle positions.

### D. Nucleon-nucleon potentials

These have the form  $V_R r^{-1} \exp(-\mu_R r) - V_A r^{-1} \exp(-\mu_A r)$ . The ranges and strengths are "reasonable" based on potentials of Bethe and Johnson,<sup>30</sup> but are adjusted to satisfy the following requirements.

1. The binding energy should be  $B \approx 8$  MeV/nucleon. It seems important to have  $B$  correctly since this, for a given laboratory energy  $E_L$ , determines how much energy is available to blow the system completely apart, i.e., to separate all the nucleons outside the range of the forces. The value of  $B = 8$  MeV is obtained by minor adjustments of the kinetic energy as already discussed. It should be remarked that it is important also to have reasonable values for the initial internal ("Fermi") kinetic energies since these can be expected to have an important effect, especially on the final (double differential) angular and energy distributions (Sec. III G). As already pointed out, our forces do not give a minimum of the energy at  $\rho_0$ . The implications of this are discussed below (especially Sec. IV B). It is our belief that this defect could perhaps be most serious for the binding of large final fragments produced in central collisions (Sec. III D).

2. Ideally, the  $N$ - $N$  differential cross sections for  $E_L \approx 50$ – $300$  MeV should be reproduced in a *classical* two-body calculation since our many-body calculations are classical. Since this seems not possible for a local potential (because of diffractive and exchange effects) we took as the most essential feature to be reproduced, in the above energy range, the cross section

$$\begin{aligned} \sigma_v &= 2\pi \int_0^\pi \sigma(\theta) \sin^2 \theta d(\cos \theta) \\ &= 2\pi \int_0^\infty \sin^2 \theta b db, \end{aligned}$$

where  $\sigma(\theta)$  is the c.m. differential cross section. The second expression may be used in a classical calculation where  $\theta = \theta(b)$  is the deflection function. On the one hand, the cross section  $\sigma_v$  is appropriate for the viscosity and thermal conductivity as determined from the Boltzmann equation for near equilibrium conditions,<sup>31</sup> while on the other hand, the viscosity is most appropriate for shock structure in a viscous-hydrodynamics description.<sup>13</sup>  $\sigma_v$  emphasizes transverse momentum transfers more strongly than the total cross section. [ $\sigma_v$  is, in fact, to a good approximation proportional to  $\sigma(90^\circ)$ .]

We did not include the Coulomb interaction or distinguish between neutrons and protons. These approximations are expected to be good at the en-

ergies and for the nuclei ( $A_1=A_2=50$ ) mostly considered. The appropriate average is then  $\bar{\sigma}_v = \frac{1}{2}[\sigma_v(np) + \sigma_v(pp)]$  with the Coulomb peak removed for  $\sigma_v(pp)$ . The empirical values are  $\bar{\sigma}_v = 86.5, 39.2, 26.5,$  and  $25.0$  mb at  $E_L = 50, 100, 200,$  and  $300$  MeV, respectively.<sup>32</sup> The corresponding calculated values are  $83.3, 42.0, 25.2,$  and  $20.5$  mb for the potential (I) which we mostly used and which has the parameter values  $\mu_A = 2.618, \mu_R = 3.990, V_A = 2040,$  and  $V_R = 7922$  ( $\mu$  in  $\text{fm}^{-1}, V$  in MeV fm.) As a measure of the repulsive core we have  $V(r) = 0$  and  $300$  MeV for  $r = 0.99$  and  $0.665$  fm, respectively. [For the Bethe-Johnson potentials the corresponding values are  $0.99$  and  $0.62$  fm for the average of their even and odd  $l$  potentials ( $l \geq 2$ ); however, their S-state potentials have considerably smaller core radii.] Another potential (II) is considered below.

It should be noted that the calculated quantum-mechanical values of  $\sigma_v$  for our potentials are, in general, considerably less than the classical values although they approach the latter at the higher energies ( $E_L \geq 250$  MeV). It should also be remembered that at lower energies the effect of the exclusion principle will be to reduce the effective cross section and to correspondingly increase the mean-free path and the transparency.

### III. RESULTS

#### A. Definitions; effects of evaporation

Most of our results are for  $A_1 = A_2 = 50$  and for the potential I quoted above, and these are the only ones we discuss except in Sec. III H. Two laboratory (relative) velocities were considered, namely,  $v = 0.5$  and  $0.8$  (velocities are relative to  $c$ ) corresponding to *nonrelativistic* energies of  $E_L \approx 117$  and  $300$  MeV/nucleon, respectively. We discuss almost only average values.

Time  $t$  is in units of  $\text{fm}/c$  ( $0.33 \times 10^{-23}$  s).  $T(t)$  denotes the "collisional" translational energy/nucleon of the c.m. motion of all the nucleons belonging initially to either nucleus in the total c.m. system.<sup>33</sup>  $I(t) = [T_i - T(t)]/T_i$  is the "inelasticity," where  $T_i \equiv T(0) = \frac{1}{2}E_L$  is the initial collisional translational energy;  $I_f$  is the final inelasticity after the collision.  $I_f = 1$  if  $T_i$  has all been dissipated during the collision.  $W(t)$  denotes the magnitude of the average potential energy/nucleon.  $F(t) = W(t)/W_i$  where  $W_i \equiv W(0)$  and  $F_f = W_f/W_i$  is the ratio of the final to the initial potential energies per nucleon.  $F_f$  is a measure of the proportion of nucleons finally bound in fragments. Thus  $W_f = F_f = 0$  if all the nucleons are finally well separated outside the range of their forces;  $F_f = 1$  if they remain bound as initially, e.g., if the two nuclei pass through each other without interaction; also  $F_f \approx 1$  if the

two nuclei completely fuse with the fused nucleus having moderate excitation energy. The final velocity asymmetry is characterized by  $\omega_f = \langle v_z^2 \rangle^{1/2} / \langle v_\perp^2 \rangle^{1/2}$ , where  $\langle v_z^2 \rangle^{1/2}$  and  $\langle v_\perp^2 \rangle^{1/2} = \langle \frac{1}{2}(v_x^2 + v_y^2) \rangle^{1/2}$  are the final values of the rms velocities in the incident and perpendicular to the incident directions, respectively.

What is meant by "final" in the above needs some explanation. This does not in general imply  $t = \infty$  because of the problems of evaporation and condensation already mentioned. Since  $T(t)$  is constant when there is no mutual interaction (and equal to  $T_i$ ) and becomes constant for the interacting case after quite short times when the collision is effectively over, the values of  $T_f$ , and hence of  $I_f$ , can be identified with  $t = \infty$ . The non-interacting values  $W_{NI}$  and  $\omega_{NI}$  of  $W$  and of  $\omega$ , respectively, vary quite slowly and are quite close to the initial values. Thus (for both  $v = 0.5$  and  $0.8$ )  $W_{NI} \approx 34$  and  $32$  MeV for  $t = 50$  and  $70$   $\text{fm}/c$ , respectively, compared with  $W_i = W_{NI}(0) = 30$  MeV; and, for  $v = 0.5$ ,  $\omega_{NI}(t = 50 \text{ fm}/c) = 2.06$  and  $\omega_{NI}(t = 70 \text{ fm}/c) = 1.99$  compared with  $\omega_i = \omega_{NI}(0) = 2.20$ . The values of  $W_f$  and  $\omega_f$  correspond to  $t_f = 50$   $\text{fm}/c$  and have been corrected by scaling, e.g.,  $W_f = W(t_f)[W_i/W_{NI}(t_f)]$  where  $W_i/W_{NI}(t_f) = 0.93$ , and similarly for  $\omega_f$ , where  $\omega_i/\omega_{NI}(t_f) = 1.07$  and  $1.06$  for  $v = 0.5$  and  $0.8$ , respectively.<sup>34</sup>

The time scale for evaporation is indicated by the variation of the (ensemble average of the) radius  $R_{50}$  of the individual nuclei. Here  $R_A = \langle \frac{5}{3} \sum_{i=1}^A r_i^2 / A \rangle^{1/2}$ , and is the root-mean-square radius of the uniform distribution with the same mean-square radius as that of the  $A (= 50)$  nucleons.  $R_{50} \approx 4.2, 4.2, 4.2, 4.8, 5.3,$  and  $6.5$  fm for  $t = 0, 10, 20, 30, 40,$  and  $50$   $\text{fm}/c$ , respectively. On the other hand, for central collisions with small  $b$  effectively all the nucleons of the two nuclei have strongly interacted when  $t \approx 30$  and  $20$   $\text{fm}/c$  for  $v = 0.5$  and  $0.8$ , respectively. The effective collision time decreases as  $b$  increases and becomes zero for very peripheral collisions with  $b \geq 2.3R$ . The time scale for evaporation is thus sufficiently longer than that of the collisions for these not to be affected significantly by the effects of evaporation.

#### B. Densities

$\rho^{(r)}(t)$  denotes the mean density inside a sphere of radius  $r$  with c.m. as origin,  $\rho_{NI}^{(r)}(t)$  is the value without mutual interaction. In all cases the initial rise of  $\rho^{(r)}(t)$  and  $\rho_{NI}^{(r)}(t)$  is almost identical (e.g., Figs. 2, 3, and 4) up to a time  $\approx 10$   $\text{fm}/c$  consistent with the mean-free path as obtained from  $\sigma_v$ . The maximum value of  $\rho^{(r)}$  is never significantly larger, for any value of  $b$ , than the maximum value of

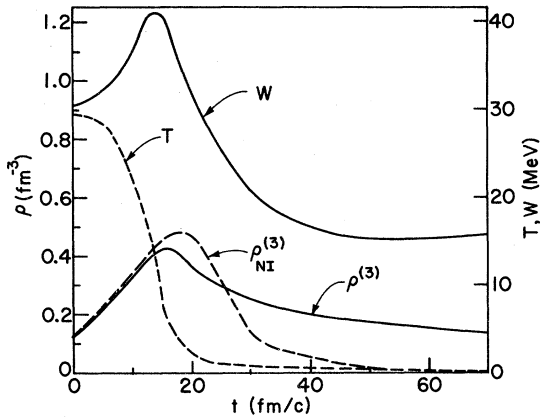


FIG. 2. Time-dependent results in the c.m. system for  $A_1=A_2=50$ ,  $v=0.5$ , and  $b=0$ .  $\rho^{(3)}$  is the average density inside a radius 3 fm with c.m. as origin;  $\rho_{NI}^{(3)}$  is the value in the absence of mutual interaction.  $W$  is the magnitude of the average potential energy/nucleon;  $T$  is the collisional translational energy/nucleon of either nucleus (see Sec. IIIA).

$\rho_{NI}^{(3)}$  which is just twice the initial central density (Fig. 5). Note that  $\rho_{NI}^{(3)}(t)$  after having reached its maximum falls off rapidly because of the increasing separation of the two noninteracting nuclei. It is seen (Fig. 4) that for larger impact parameters the values of  $\rho(t)$  and  $\rho_{NI}(t)$  are almost identical, indicative of rather little mutual interaction.

### C. Central collisions ( $b \leq R$ )

These are "explosive." After an initial weakly interacting, or "transparent" stage lasting about 10 fm/c, the initial collisional translational energy

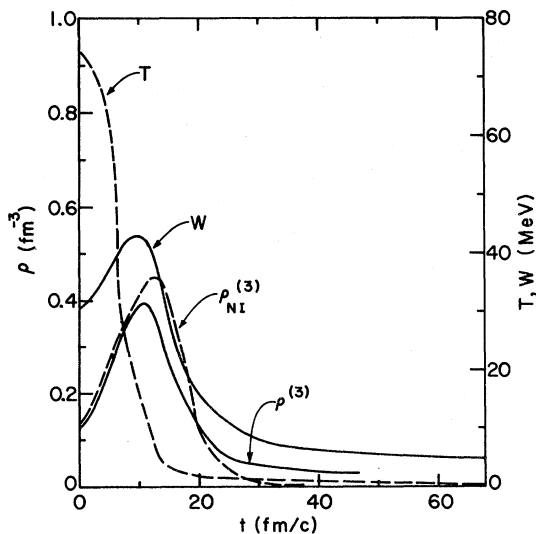


FIG. 3. As for Fig. 2 but for  $v=0.8$ .

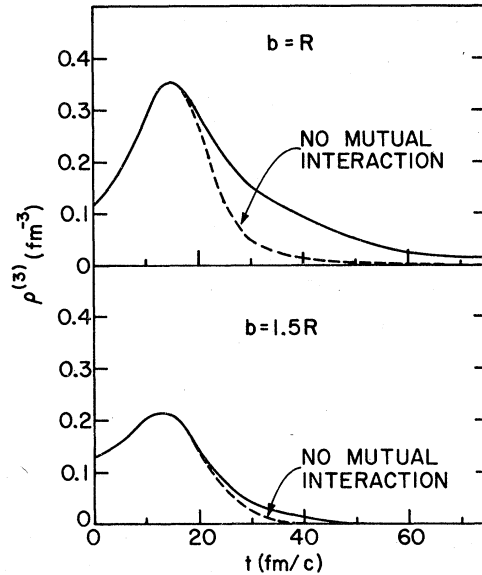


FIG. 4. The density  $\rho^{(3)}$  in the c.m. system (see caption for Fig. 2), for  $A_1=A_2=50$  and for  $b=R$  and  $1.5R$  as a function of time.

$T_i$  is rapidly dissipated and randomized during a short "critical" period of about 5 fm/c, of the order of  $\Lambda/v$ , when the  $A$  nucleons become completely intermingled (Fig. 6) with high internal energies at maximum compression (Figs. 2, 3, and 6). Subsequently, in the final stage, there is an explosive expansion involving large, approximately radial, velocities. This is illustrated by Fig. 6 which shows, for  $v=0.5$ , the radius  $R_A$  for the whole system ( $A=100$ ) vs  $t$ , where  $R_A$  was defined above. For both  $v=0.5$  and  $0.8$  one has  $dR_A/dt \approx \frac{1}{2}v$  in the final stage, corresponding to final velocities consistent with an explosive final stage.<sup>35</sup> Furthermore, as discussed below, there are a substantial number of nucleons with final speeds significantly greater than  $0.5v$ .

For  $A_1=A_2=50$  the final angular distributions

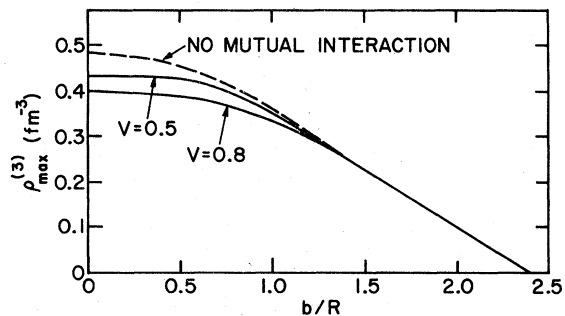


FIG. 5. The maximum density  $\rho_{\max}^{(3)}$  attained during a collision vs  $b/R$  for  $A_1=A_2=50$ .

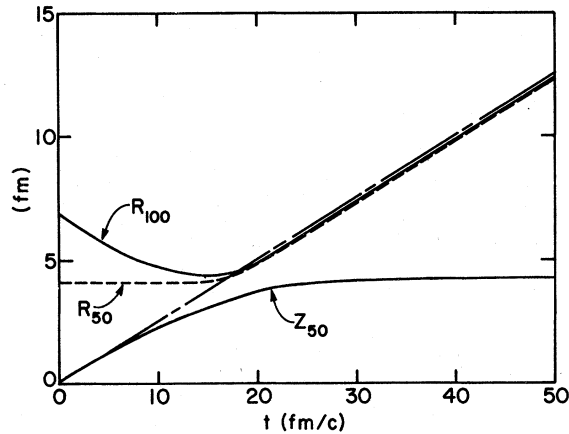


FIG. 6. Time-dependent results in the c.m. system for  $A_1=A_2=50$  and  $v=0.5$ .  $R_{50}$  denotes the radius of the equivalent uniform distribution (see Sec. III A) of the nucleons belonging to either initial nucleus,  $R_{100}$  the corresponding radius for all the nucleons.  $Z_{50}$  denotes the displacement, in the incident direction, of the c.m. of the nucleons belonging to either initial nucleus; the straight dash-dotted line represents the displacement if the nuclei continue moving with their initial velocity (0.25 in the c.m. system). Note that  $R_{50}$  and  $R_{100}$  become equal at  $t \approx 15$  fm/c, indicating that the nucleons from the two nuclei have then become completely intermingled. Note also that  $Z_{50}$  becomes constant for  $t \gtrsim 20$  fm/c, consistent with all the initial collisional translational energy  $T_{\dot{z}}$  having been dissipated.

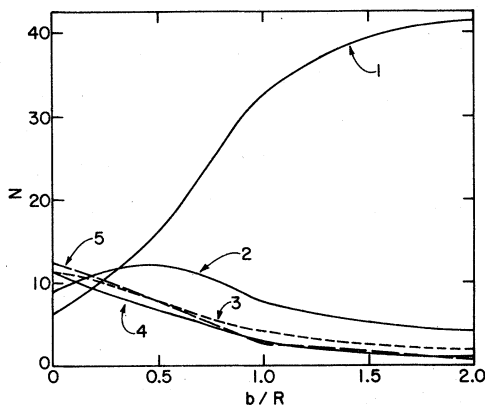


FIG. 7. Angular distributions in the c.m. system for  $A_1=A_2=50$  and for  $v=0.5$  for nucleons of all final velocities vs  $b/R$ . The labels 1, ..., 5 denote the following intervals of  $\cos\theta$ : 1-0.8 (1), 0.8-0.6 (2), 0.6-0.4 (3), 0.4-0.2 (4), 0.2-0 (5).  $N$  denotes the number of nucleons, the normalization being such that the total number of nucleons for  $0 \leq \cos\theta \leq 1$  is 50 for each value of  $b/R$ . The values for Figs. 7, 8, 11, and 12 are averages over the corresponding forward and backward intervals, the angular distributions being symmetrical about  $90^\circ$  to within the expected small fluctuations.

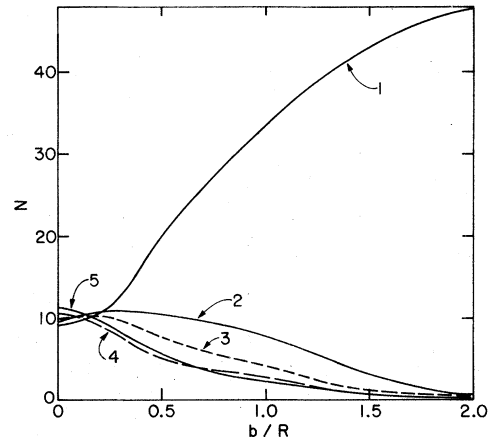


FIG. 8. As for Fig. 7 but for  $v=0.8$ .

are roughly isotropic for  $b \lesssim 0.3R$  as shown by Figs. 7 and 8 which show the angular distributions vs  $b/R$ . The same feature is also indicated by the results for the final velocity asymmetry  $\omega_f$  vs  $b/R$  (Fig. 9). For small  $b$  one has  $\omega_f \approx 1$ , indicating approximate isotropy of the final distributions. However, it is important to note, as shown by Figs. 7 and 8 that even for small  $b$  there are significant deviations from isotropy and that these deviations change quite rapidly with  $b$ . Thus for very small  $b$ , and in particular for  $b=0$ , there is a "sideways" or transverse peaking of the angular distribution with  $\sigma(90^\circ)/\sigma(0^\circ) \approx 2$  and 1.3 for  $v=0.5$  and 0.8, respectively. This is reminiscent of some hydrodynamic predictions.<sup>3,8</sup> However, even for quite small  $b \approx 0.2R$ , this sideways peaking changes over to a forward peaking which becomes quite pronounced for  $b \gtrsim 0.5R$ . Since it is the small impact parameters which are associated with

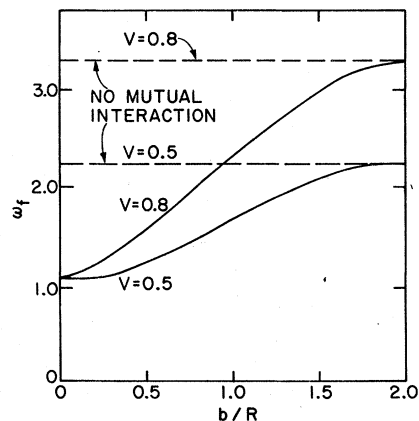


FIG. 9. The velocity asymmetry  $\omega_f = \langle v_z^2 \rangle^{1/2} / \langle v_{\perp}^2 \rangle^{1/2}$  in the c.m. system vs  $b/R$  for  $A_1=A_2=50$ ;  $\omega_f$  has been corrected as in Sec. III A.

large compressions and shock-type phenomena, it may thus be necessary to have quite detailed information about the angular distributions as a function of  $b$  in order to obtain significant information about the equation of state.<sup>36</sup>

The general behavior so far discussed is quite similar for  $v=0.5$  and  $0.8$ . For central collisions, on the average, enough of the nuclei traverse each other, relative to the mean-free path, that these collisions seem fairly well equilibrated at the stage of maximum compression and subsequently. Consistent with this is also a large relative dispersion of  $T_f$  and  $W_f$  for the central collisions. The density, although conditions do become fairly well equilibrated in central collisions, never appreciably exceeds the maximum density without mutual interaction (i.e.,  $2\rho_0$ ) and is considerably less than the density expected for a fully developed shock (i.e., not too much less than the  $4\rho_0$  for an ideal monoatomic gas, in view of the rather small repulsive core).

#### D. Fusion

A notable difference between  $v=0.5$  and  $0.8$  is that for  $v=0.5$  there is considerable fusion for  $b \leq 0.5R$ , involving a fused residue of about 50–70 nucleons, whereas for  $v=0.8$  there are no large final fragments, but only indications of a few smaller ones. Final here means  $t \approx 30\text{--}70 \text{ fm}/c$ . (For large times, the effects of condensation and evaporation will become substantial.) By fusion we do not necessarily imply a fused residue of mass  $A$  but only a persistent residue of appreciable mass number and reasonable density, which may be moderately excited and is approximately at rest in the total c.m. system.

The fused residues are indicated very clearly by the results for the populations and density (in both cylindrical and spherical polar coordinates) and by the corresponding values of the internal energy. By inspection of the results for the population one may also readily estimate the mass of the residues. Since the residues are "observed" at a time of order of the collision time  $\tau_{\text{col}}$  and since they are excited (by several MeV/nucleon) evaporation will occur (on a longer time scale than  $\tau_{\text{col}}$ ). The final asymptotic fragments would therefore have a smaller mass than those we "observe."

The presence of the fused residue is reflected and supported by the behavior of  $\rho^{(r)}(t)$  and  $W(t)$ . Thus even allowing for the fact that to a first approximation the collision for  $v=0.5$  proceeds only  $\frac{5}{8}$  as fast as that for  $v=0.8$ , the falloff of  $\rho^{(r)}(t)$  is much slower for  $v=0.5$  than for  $v=0.8$  (Figs. 2 and 3). This is because the fused residue is approximately at rest in the c.m. system and

leads to a persistence in  $\rho^{(r)}(t)$ . The quantity  $F_f = W_f/W_i$  is, as already mentioned, an indication of the proportion of nucleons finally bound in fragments. Figure 10 shows that for  $v=0.8$  one has  $F_f \approx 0.15$  for  $b \leq 0.5R$ , consistent with only a few small final fragments. However, for  $v=0.5$  one has  $F_f \approx 0.55$ , reflecting substantial fused residues. The total fusion cross section for  $v=0.5$  is fairly small ( $\leq 100 \text{ mb}$ ) because fusion occurs only for small  $b$ .

That there is less fusion at higher energies may be understood most simply because more energy is then available to blow the system apart. (For both energies collisions with small  $b$  are highly inelastic, i.e.,  $I_f \approx 1$ , and  $T_i$  is effectively all dissipated). Nevertheless, it seems surprising that even for  $v=0.5$  there is any substantial fusion, since  $T_i \approx 30 \text{ MeV}$  is much larger than the binding energy. Since during the "critical" period the system is highly excited, there must be some mechanism by which a substantial number ( $\approx 60$ ) of nucleons can very rapidly lose much or even most of their energy to the other nucleons and finally remain as a fused fragment. We conjecture that this can occur because for small  $b$  the central parts of the nuclei interact somewhat earlier and also thermalize more completely (because the relevant dimensions are larger relative to the mean-free path) than the outer parts and, moreover, are perhaps "held in place" to some extent by the latter. This may then allow the inner nucleons to lose their energy sufficiently rapidly (via heat conduction) to the outer nucleons to enable the inner nucleons to remain as a fused residue, the outer nucleons being explosively blown off. It should be noted that the unfused nucleons are blown off with explosive velocities

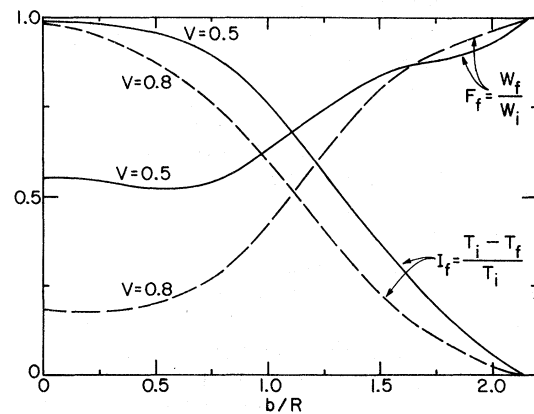


FIG. 10. The inelasticity  $I_f$  and the ratio  $F_f$  vs  $b/R$  for  $A_1 = A_2 = 50$ .  $W_i$ ,  $T_i$  are the initial values;  $T_f$ ,  $W_f$  are the final values after the collision;  $W_f$  has been corrected as discussed in Sec. IIIA.

as indicated by the final value of  $dR_A/dt$  of about 0.25 (Fig. 6) and also by the large number of final nucleons with velocities greater than 0.25 (Sec. III G).

Although our forces give the correct binding at normal densities, they do not give a minimum of the energy (as a function of  $\rho$ ) at  $\rho_0$ , i.e., they do not give the correct "saturation properties." However, we believe that our conclusions about the occurrence of fused residues are significant since these residues do have a reasonable binding energy ( $\approx 3$  MeV/nucleon) and density ( $\approx 0.15$  fm $^{-3}$ ). Of course, it would clearly be most desirable to have forces with more adequate "saturation properties." It is, however, a highly nontrivial problem to reconcile these properties with adequate scattering properties and reasonable repulsive cores. These and related problems are discussed further, especially in Sec. IV B. In any case, our results show that there is an efficient mechanism for the rapid cooling of a large number of nucleons in central collisions.

#### E. Noncentral (peripheral) collisions ( $b \geq R$ )

These are nonexplosive and much less dramatic than those for small  $b$ . Less of the initial collisional translational energy is lost than for central collisions and  $I_f$  is considerably less than unity (Fig. 10).  $W(t)$  varies less with  $t$  and the differences between  $\rho$  and  $\rho_{NI}$  are much less than for small  $b$  (Fig. 4). For larger  $b$  there is increasing persistence of the initial velocities and the two nuclei increasingly retain their identity and increasingly remain intact. Thus for  $v=0.8$  already for  $b \approx R$  (and even somewhat less) about 40 nucleons of each nucleus "finally" remain together, whereas for  $b \approx 1.5R$  the "final" nuclei have lost only about five nucleons each. This is also consistent with the values of  $F_f$  (Fig. 10). Thus  $F_f$  is large for  $b \geq R$  and approaches unity for  $b \approx 2R$ . For very peripheral collisions with  $b \geq b_{\max} \approx 2.3R$  there is no mutual interaction and  $F_f = 1$ . Similar remarks apply for the long-time behavior of the fragments produced in peripheral collisions as for the fused residues formed in central collisions. Thus the fragments which we "observe" at times of the order of  $\tau_{\text{col}}$  and which are excited may be termed prefragments in the terminology of Hüfner (Ref. 22). The actual final fragments will result from these prefragments by evaporation and will have smaller masses.

The increasing persistence of the initial velocities for larger  $b/R$  is illustrated in Fig. 9; thus the final velocity asymmetry  $\omega_f$  approaches the no mutual-interaction value for large  $b$ . Another aspect of this (Figs. 7 and 8) are the increasingly

forward peaked angular distributions (of nucleons of all final kinetic energies) for larger  $b$ . It is to be noted that although the mass loss is relatively small, the inelasticities are quite large for  $R \lesssim b \lesssim 1.5R$ .

Nonequilibrium and transparency effects are seen to develop quite rapidly with increasing  $b$ , as is evident from, e.g., the dependence on  $b$  of the inelasticity  $I_f$  and of the angular distributions. On the average, so little of the nuclei traverse each other that only quite partial ( $b \approx R$ ) or almost no equilibrium ( $b \geq 1.5R$ ) is attained; the nuclei retain much or most of their identity suffering relatively little mass loss and the relative dispersion, e.g., of  $T_f$ , is much less than for small  $b$ . Clearly, the final state has little resemblance to equilibrium conditions for  $b \geq R$ . However, the inelasticities are still very appreciable even for quite large values of  $b$ ; in particular the appropriately weighted values (i.e.,  $bI_f$ ) peak around  $b \approx R$ . Compressibility phenomena are hardly apparent for larger  $b$  ( $\geq R$ ).

#### F. Inelasticity and transparency

$I_f$  is consistently less for  $v=0.8$  than for 0.5 for all  $b$  (Fig. 5). A measure of the average inelasticity is  $\bar{I}_f = \int_0^{b_{\max}} I_f b db / \int_0^{b_{\max}} b db$ . ( $\bar{I}_f = 1$  if  $I_f = 1$  for all  $b$ .)  $I_f b$  peaks at  $b \approx R$ . For  $v=0.5, 0.8$ , one obtains  $\bar{I}_f = 0.41, 0.32$ , respectively. The decrease of  $I_f$  and  $\bar{I}_f$  with increasing energy is consistent with the expected greater transparency (smaller  $\sigma_v$  and viscosity) at higher energies.<sup>37</sup> This increasing transparency is also consistent with the following results. The final velocity asymmetry  $\omega_f$  (Fig. 9) increases more rapidly with increasing  $b$  for  $v=0.8$  than for  $v=0.5$ . [Recall that  $\omega_f \approx 1$  corresponds to complete randomization of the initial incident velocity and  $\omega_f = \omega(0)$  to complete transparency.] The angular distributions (Figs. 7 and 8) become more rapidly forward peaked as a function of  $b/R$  for  $v=0.8$  than for  $v=0.5$ .

It should be remembered that the exclusion principle will be more effective in reducing in  $N-N$  cross sections, and thus also  $\sigma_v$ , at lower energies. Since this will lead to a relatively greater increase of transparency at lower energies, the net effect is expected to reduce the differences in transparency between  $v=0.5$  and 0.8.

#### G. Angular distributions

The c.m. angular distributions of nucleons of all final energies as a function of  $b/R$  (Figs. 7 and 8) have already been discussed. Angular distributions are obtained by integrating such distributions over  $b$  (with weighting proportional to  $b$ ). Figure 11 shows results for  $0 \leq \cos\theta \leq 1$  for

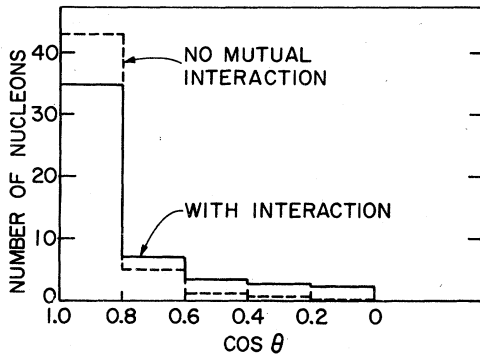


FIG. 11. Angular distribution in the c.m. system for  $A_1=A_2=50$  and  $v=0.5$  for nucleons of all final velocities. Shown are the number of nucleons in intervals of 0.2 of  $\cos\theta$  for  $0 \leq \cos\theta \leq 1$ , and normalized to a total number of 50.

$v=0.5$ . The values are averages of the numbers in the corresponding forward and backward angular intervals, the angular distribution being in fact symmetric about  $90^\circ$  to within the expected small fluctuations. The angular distributions correspond to  $t_f \approx 50$  and  $70$  fm/c for  $v=0.8$  and  $0.5$ , respectively. Because the size of the individual noninteracting nuclei increase with  $t$  due to evaporation, the angular distributions without mutual interaction spread out of the forward direction. (Recall that the angular distributions are obtained from the particle positions and not the velocities.)

Comparison with the results for no mutual interaction then shows that the large forward (and backward) peaking in the overall c.m. angular distribution is due to the relatively minor effect of the collision for the heavily weighted large- $b$  collisions. The most interesting part is thus the large-angle distribution which has important contributions from the small- $b$  "explosive" collisions.

Table I shows the c.m. angular distributions for three ranges of  $v_f/v$  where  $v_f$  is the final radial nucleon velocity. The values are normalized to 50 for nucleons with  $v_f \geq 0$  (also equal to the number of nucleons of all final energies) and  $0 \leq \cos\theta \leq 1$ . The scattering is more forward peaked for  $v=0.8$  than for  $0.5$  for all ranges of  $v_f$ , consistent with greater transparency at the higher energy. Comparison with the no-mutual-interaction values shows that there is a significant and appreciable flux of high-velocity nucleons (with  $v_f \geq 0.5v$  and even with  $v_f \geq 0.7v$ ) at large angles (arising from central collisions). The initial internal ("Fermi") kinetic energy seems an important factor for these high-velocity nucleons. Thus there is a smaller number of nucleons with large  $v_f/v$  (e.g.,  $\geq 0.7$ ) for  $v=0.8$  than for  $v=0.5$ , since for a (fixed) Fermi velocity  $v_F$  ( $\approx 0.3$ ) given values of the ratio  $v_f/v$  are closer to  $(0.5v + v_F)/v$  for  $v=0.8$  than for  $v=0.5$ . [Thus for  $v_f > (0.5v + v_F)$  the flux is expected to be zero in the absence of multiple scattering effects. These latter could give final speeds greater than  $0.5v + v_F$ .]

TABLE I. Number of nucleons in the c.m. system, for  $A_1=A_2=50$ , in intervals of 0.2 of  $\cos\theta$  and for three ranges of  $v_f/v$ , where  $v_f$  is the final radial nucleon velocity and  $v$  the laboratory velocity. The numbers are averages over the corresponding forward and backward intervals and are normalized to 50 for the number of nucleons of all  $v_f$  in the range  $0 \leq \cos\theta \leq 1$ . Int. denotes the actual interacting case, No Int. the case of no mutual interaction.

$\cos\theta$	$N(0 \leq v_f/v \leq 0.5)$		$N(0.5 \leq v_f/v \leq 0.7)$		$N(v_f/v \geq 0.7)$	
	Int.	No Int.	Int.	No Int.	Int.	No Int.
$v=0.5$						
1-0.8	18.78	20.54	9.26	11.23	6.83	11.26
0.8-0.6	3.40	2.12	1.88	1.68	1.31	1.10
0.6-0.4	2.13	0.67	0.82	0.19	0.53	0.39
0.4-0.2	1.49	0.56	0.59	0.19	0.52	0.00
0.2-0	1.56	0.7	0.50	0.00	0.42	0.00
1-0	27.36	23.96	13.05	13.29	9.59	12.75
$v=0.8$						
1-0.8	21.47	24.21	13.37	18.20	4.01	4.77
0.8-0.6	2.95	1.26	1.29	0.76	0.44	0.37
0.6-0.4	1.81	0.31	0.69	0.11	0.18	0.00
0.4-0.2	1.22	0.00	0.55	0.00	0.24	0.00
0.2-0	1.21	0.00	0.41	0.00	0.15	0.00
1-0	28.66	25.78	16.31	19.07	5.02	5.14

#### H. Results for other potentials and for $A_1 = A_2 = 200$

We discuss some (much less complete) results for some other potentials and also for  $A_1 = A_2 = 200$  which are of interest.

Another potential (II) which we used for  $A_1 = A_2 = 50$  also gives  $B = 8$  MeV and similar values for  $\sigma_v$  as does potential I which was considered previously; however, II has a repulsive core about 0.05 fm larger than I. Thus the transport and collisional relaxation properties should be similar for both potentials. The parameters of II are  $V_A = 2570$ ,  $V_R = 7057$  (MeV fm),  $\mu_A = 2.402$ ,  $\mu_R = 3.328$  (fm<sup>-1</sup>), and the values of  $\sigma_v$  are 88.4, 44.9, 28.1, and 23.2 mb for  $E_L = 50, 100, 200,$  and 300 MeV, respectively.  $V(r) = 0$  and 300 MeV for  $r = 1.09$  and 0.70 fm, respectively.

Calculations with II were made for  $v = 0.5$  and 0.8 but for only two impact parameters,  $b = 0$  and  $R$ . The corresponding results for I and II are generally quite similar but show some interesting and suggestive differences. The inelasticities  $I_f$  are very similar for I and II. Since the inelasticities are presumably mainly determined by the viscosity, this result is consistent with the similar values of  $\sigma_v$  for I and II. The values of  $W_f$  and hence of  $F_f = W_f/W_i$  are quite similar for I and II, but somewhat smaller for II. For II when  $v = 0.5$  one again has  $F_f \approx 0.5$  for  $b \lesssim 0.5R$ ; also, for  $b = 0$ ,  $\rho^{(3)}(t)$  again shows the same persistent behavior as for I. Both these features are again consistent with substantial fusion for  $v = 0.5$ , whereas for  $v = 0.8$ , just as for I, there is no indication of any substantial final fragments.

The values of  $\rho_{\max}^{(3)}$  for II are less by about 0.25 fm<sup>-3</sup> (for both  $b = 0$  and  $R$ ) than those for I (shown in Fig. 5). This is consistent with the larger repulsive core for II. The values of the velocity asymmetry  $\omega_f$  are generally very similar but are slightly less for II, especially for  $b = 0$ ; thus  $\omega_f(b = 0) = 0.96$  for II instead of 1.06 as for I, implying that the final transverse velocities are somewhat greater than those along the incident direction, reminiscent of hydrodynamic predictions. The c.m. angular distributions for both  $b = 0$  and  $R$  are very close for I and II when  $v = 0.5$ . However, for  $v = 0.8$  there are some moderate but significant differences, especially for  $b = 0$  for which there is more pronounced sideways peaking for II; thus  $\sigma(90^\circ)/\sigma(0^\circ) \approx 1.9$  for II as compared with 1.3 for I; this is consistent with the results for  $\omega_f$ .

We also made some exploratory calculations for the extreme case of a Lennard-Jones potential with a very large and steep repulsive core, and which gives a very incompressible liquid of closely packed nucleons with density  $\rho_0$  and  $B = 8$  MeV.

For  $A_1 = A_2 = 50$ ,  $v = 0.5$ , and  $b = 0$  the collision then has the splashing features expected in a head-on collision of two incompressible drops; thus transverse jets develop very rapidly and there are no noticeable transparency effects and no appreciable increases in density.

For  $A_1, A_2 > 50$  shock phenomena may be more prominent relative to transparency effects because the nuclear dimensions then become larger relative to the mean-free path. Some of our first rather preliminary calculations are pertinent to this question. These were for  $A_1 = A_2 = 200$ ,  $v = 0.8$ , and  $b = 0$  but for a potential which gives somewhat *too small* values for  $\sigma_v$ , and hence somewhat too large  $\Lambda$ . It is noteworthy that in spite of this, the c.m. angular distribution (Fig. 12) shows a strong sideways peaking with  $\sigma(90^\circ)/\sigma(0^\circ) \approx 3$  and the maximum densities are about  $3\rho_0$ . Both these features indicate possibly a more fully developed shock situation than for  $A_1 = A_2 = 50$ ; however, this must be qualified by the fact that the repulsive core is somewhat smaller than for potential I.

#### IV. DISCUSSION, PROBLEMS AND EXTENSIONS

##### A. Transparency and hydrodynamic phenomena

For small impact parameters  $b$ , i.e., for central collisions, there is some similarity with the development of shocks: "explosive" collisions with

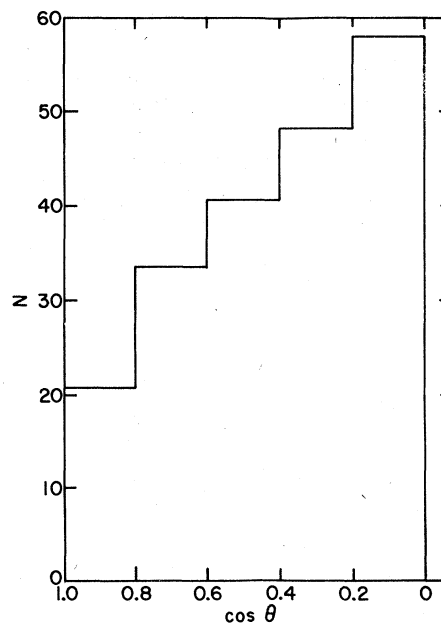


FIG. 12. Angular distribution in the c.m. system for  $A_1 = A_2 = 200$ ,  $v = 0.8$  and  $b = 0$ .  $N$  denotes the number of nucleons in intervals of 0.2 of  $\cos \theta$ , normalized to a total number of 200.

an initial weakly interacting (transparent) stage; subsequent rapid and almost complete randomization of the translational energy during a time interval of the order of  $\Lambda/v$  ( $\approx 5-10$  fm/c), and associated large compressions and internal energies, with finally an explosive expansion; the c.m. angular distribution is roughly isotropic for small  $b$  but shows some characteristic transverse peaking for very small  $b$ . Thus for central collisions, on the average, enough of the nuclei traverse each other, relative to the mean-free path, that these collisions seem fairly well equilibrated at the stage of maximum compression and subsequently.

Nonequilibrium and transparency effects develop quite rapidly with increasing  $b$ , as is evident from, e.g., the dependence of the inelasticity and the angular distributions on  $b$ . On the average so little of the nuclei traverse each other that only quite partial ( $b \approx R$ ) or almost no equilibrium ( $b \approx 1.5R$ ) is attained; the nuclei retain much or most of their identity suffering relatively little mass loss. However, the inelasticities are still very appreciable even for quite large values of  $b$ . Compressibility effects are hardly apparent for larger  $b$  ( $\geq R$ ). Clearly, the final state has little resemblance to equilibrium conditions for  $b \geq R$ .

Significant information about the equation of state must presumably come from the "explosive" central collisions. Since our calculations show, at least for  $A_1 = A_2 = 50$ , that mean-free path effects have an important effect even for small  $b$ , this will make it considerably more difficult to obtain information about the equation of state than is suggested by hydrodynamic considerations. In particular, our results suggest that it will be necessary to determine the (rather strong) dependence of the angular distributions on the impact parameter for quite small impact parameters. Since  $b$  is not directly observable it may be quite difficult to obtain this from experiment.<sup>36</sup>

Significant information about transport coefficients may, in fact, be more readily obtainable than information about the equation of state. Thus, e.g., the viscosity may be determinable from the inelasticity and its dependence on  $b$ . Of particular interest is the possibility of large fused residues whose properties and production cross section may be relevant for the thermal conductivity.

Our present results cannot be directly compared with experiment—in particular because of the energies and nuclei we have considered. However, some features of our results show a strong resemblance to aspects of the data.

Thus our noncentral nonequilibrated collisions have a strong general resemblance to the fragmen-

tation collisions at GeV/nucleon energies. These collisions are characterized by large transparency (persistence of projectile and target) with an average overlap distance between the nuclei of about 2 fm and associated properties of factorization and limiting fragmentation.<sup>15</sup> In fact, our more peripheral collisions, for which we found only slight mutual interaction in our calculations, correspond to  $b \approx 1.5R$  which with  $R \approx 4$  fm (for  $A = 50$ ) just gives an overlap distance of about 2 fm. A Glauber-approximation treatment (Ref. 22) seems to give a reasonable description of these collisions and such a treatment is closely related to classical microscopic approaches, in particular to the cascade and Boltzmann-equation approaches, for large transparencies, i.e.,  $\Lambda > L$  (Sec. IC). There is also evidence (for  $^{16}\text{O} + ^{208}\text{Pb}$ ) of nonequilibrated peripheral collisions at lower (but not too low) energies of about 20 MeV/nucleon.<sup>38</sup> The relative cross sections for the production of various final nuclei are surprisingly similar to those at 2.1 GeV/nucleon, strongly suggestive of a common reaction mechanism for the whole span of energies. (However, at still lower energies, not far above the Coulomb barrier, the reaction mechanism seems to be quite different and to be determined by partial equilibrium phenomena, e.g., Ref. 39).

In future calculations it will clearly be of great interest to obtain the distribution of mass and momentum of the final fragments as well as of their average loss of momentum (with respect to the appropriate initial nucleus) and to compare such results with experimental ones.

Explosive-type central collisions have been seen both at energies of a few hundred MeV/nucleon as well as at GeV/nucleon energies.<sup>40</sup> There is evidence<sup>38</sup> that the cross section for these central collisions is about the same as at much lower (20 MeV/nucleon) energies (and also agrees with the high-energy limit for the estimated fusion cross sections—the equilibrated fusion reactions at lower energies presumably correspond to the equilibrated explosive collisions at higher energies).

#### B. Problems and extensions of the equations-of-motion approach

We discuss some of the more fundamental limitations of our calculations and possible ways of overcoming these.

At higher energies ( $\geq 250$  MeV/nucleon) relativistic effects are expected to become significant. The problem is that there is no unique way of including retardation effects for a static potential unless some assumptions are made about the field-theoretic origin of the potential.<sup>41</sup> An ap-

proach currently being investigated<sup>42</sup> is to consider the short-range repulsive Yukawa potential to be due to a vector field ( $\omega$ -meson field) and the longer-range attractive potential to be due to a scalar field ( $\sigma$ -meson field). The effects of retardation to order  $v^2/c^2$  are then uniquely determined in terms of the static potential.<sup>43</sup> No additional parameters are introduced, but the parameters ( $V_A, \mu_A, V_R, \mu_R$ ) of the potential inclusive of retardation corrections must, of course, be re-adjusted to fit the cross section  $\sigma_v$ .

Also at higher energies ( $\geq 400$  MeV/nucleon lab energies) pion production is expected to become important. Pions could perhaps be included in an EOM approach on lines used in cascade calculations (via  $\Delta$  production and decay and  $\Delta$ - $N$  interactions).<sup>44</sup>

We remark that both hydrodynamics and cascade calculations can readily be made relativistic. In particular, cascade calculations can readily include relativistic kinematics and particle production.

The neglect of quantum-mechanical effects especially for the equation of state could be an important limitation. We recall that hydrodynamics, although classical, can include important quantum-mechanical effects through its use of the equation of state. In particular, this ensures a reasonable compressibility and sound velocity near the normal density  $\rho_0$ . However, the role of the equation of state is not so clear in the absence of local thermodynamic equilibrium and thus especially for the initial stages of central collisions, or for most or all of noncentral collisions. A more adequate equation of state may, in fact, be most important for a better description of large final fragments (such as we found for  $v=0.5$  in central collisions).

There are several possibilities for obtaining a more adequate equation of state within the framework of EOM calculations. One is the use of momentum-dependent potentials,<sup>45</sup> or possibly of three (or more) body forces. A problem is that of maintaining both a reasonable repulsive core as well as the scattering properties necessary for an adequate description of the collisional relaxation properties.

Another approach which, in principle, can distinguish between the effect of the forces on the equation of state and on the relaxational properties, is to include degeneracy effects and other possible modifications of the equation of state via pressure-type (i.e., one-body) forces of the form  $-\vec{\nabla}_i p$  (per unit mass on the  $i$ th nucleon) where  $p(\rho)$  (which may also depend on momentum and the thermal excitation energy) is chosen to reproduce the required equation of state. Exploratory cal-

culations for spherical distributions show that pressure-type forces are capable of giving qualitatively reasonable effects.<sup>46</sup> There are two fundamental problems with this type of term. Firstly, one must be able to make a reasonable separation between the two-body forces and the average-field effects represented by the one-body pressure terms; in particular, one must avoid "double counting." Furthermore, for heavy-ion collisions the one-body terms must allow for the effects of the relative momentum of the two nuclei (especially in the initial stages of the collision) and for excitation of the nuclear matter (especially for the later stages of central collisions). These problems are clearly related to that of the role of the equation of state in heavy-ion collisions. It should be noted that pressure-type terms have their equivalent in the Boltzmann-equation or cascade approaches. Thus in cascade calculations,<sup>20</sup> they occur through the use of a single-particle potential (usually related to the density in a simple way to achieve approximate self-consistency), while in the Boltzmann equation they occur through a corresponding force term.<sup>47</sup>

Classical descriptions cannot adequately—if at all—describe the behavior for times much longer than  $\tau_{\text{col}}$ . This long-time behavior, associated with evaporation, relates the fragments formed immediately after the collision (i.e., the "prefragments") with the final nuclei to be identified with the experimentally observed ones. This long-time behavior must be obtained by special considerations, e.g., on the lines of Hüfner *et al.* (Ref. 22) involving use of evaporation-type calculations.

The light composites ( $A=2, 3$ , and 4) observed in central collisions also cannot be obtained from a classical approach. Fortunately, it seems that the cross sections for these composites can be related to the cross sections for the nucleons (which is effectively what classical descriptions can calculate) by use of a simple phenomenological, one-parameter, momentum-space coalescence model.<sup>40</sup>

We remark that if an adequate description of heavy-ion collisions should need the full solution of the quantum-mechanical  $N$ -body problem (possibly relativistic) then it would seem almost hopeless to obtain a theoretical understanding of such collisions. At higher energies ( $\geq 100$  MeV/nucleon) an essential simplification is the possibility of a classical description. Because of large transparency effects, a microscopic description (EOM or Boltzmann-equation and cascade approaches) is needed for a unified description of both central and peripheral collisions. We recall the twofold role of the nuclear forces—for the equation of state and for the relaxational processes—and that

among classical descriptions only the equations-of-motion approach, or a modified cascade approach such as that of Ref. 19, can hope to include both roles.

Finally, we remark that energies in the few hundred MeV/nucleon range seem particularly interesting. Thus on the one hand they are sufficiently high that compressional effects can be expected to be large and thus that hot dense nuclear matter can be obtained in central collisions, and that, furthermore, classical considerations are expected to be approximately valid. On the other hand, such energies are still low enough that relativistic and pion-production effects may be rela-

tively unimportant and that a theoretical understanding in terms of more-or-less conventional low-energy concepts, in particular that of nuclear forces, may still be possible.

We are greatly indebted to A. Rahman for introducing us to the computational techniques of molecular dynamics and for much help in the initial stages of this work. We are grateful to J. Boguta, A. S. Goldhaber, H. H. Gutbrod, E. C. Halbert, H. H. Heckman, A. S. Kerman, A. D. MacKellar, J. R. Nix, D. K. Scott, R. K. Smith, W. J. Swiatecki, and L. Wilets for discussions, helpful suggestions, and communications concerning this work.

\*Work supported by the U. S. Energy Research and Development Administration, Division of Physical Research.

<sup>1</sup>A. E. Glassgold, W. Heckrotte, and K. M. Watson, *Ann. Phys. (N.Y.)* **6**, 1 (1959).

<sup>2</sup>G. F. Chapline, M. H. Johnson, E. Teller, and M. S. Weiss, *Phys. Rev. D* **8**, 4302 (1973).

<sup>3</sup>W. Scheid, H. Müller and W. Greiner, *Phys. Rev. Lett.* **32**, 741 (1974); J. Hofmann, W. Scheid, and W. Greiner (unpublished).

<sup>4</sup>H. G. Baumgardt, J. U. Schott, Y. Sakamoto, E. Schopper, H. Stöcker, J. Hofmann, W. Scheid, and W. Greiner, *Z. Phys.* **A273**, 359 (1975).

<sup>5</sup>C. Y. Wong and T. A. Welton, *Phys. Lett.* **49B**, 243 (1974).

<sup>6</sup>M. I. Sobel, P. J. Siemens, J. P. Bondorf, and H. A. Bethe, *Nucl. Phys.* **A251**, 502 (1975).

<sup>7</sup>A. A. Amsden, G. F. Bertsch, F. H. Harlow, and J. R. Nix, *Phys. Rev. Lett.* **35**, 905 (1975).

<sup>8</sup>Y. Kitazoe, M. Sano, and H. Toki, *Nuovo Cimento Lett.* **13**, 139 (1975); Y. Kitazoe and M. Sano, *ibid.* **14**, 400 (1975); *Prog. Theor. Phys.* **54**, 922, 1574 (1975); Y. Kitazoe, K. Matsuoka, and M. Sano, *Formation and Disintegration of High-Density Nuclear Matter in Heavy-Ion Collisions*, Osaka University Report, 1976 (unpublished).

<sup>9</sup>J. Hofmann, H. Stöcker, U. Heinz, W. Scheid, and W. Greiner, *Phys. Rev. Lett.* **36**, 88 (1974).

<sup>10</sup>A. R. Bodmer, *Phys. Rev. D* **4**, 1601 (1971); in *The Nuclear Many-Body Problem*, edited by F. Calogero and C. Ciofi degli Atti (Editrice Compositori, Bologna, 1973), p. 509.

<sup>11</sup>T. D. Lee and G. C. Wick, *Phys. Rev. D* **9**, 2291 (1974); *Rev. Mod. Phys.* **47**, 267 (1975).

<sup>12</sup>Since the nuclei slow down relative to each other during the collision, one, in fact, expects a spread in velocities, and the Mach-cone features of the angular distributions to be correspondingly smeared out.

<sup>13</sup>See, e.g., Y. B. Zel'dovich and Yu. P. Raizer, *Elements of Gasdynamics and the Classical Theory of Shock Waves* (Academic, New York, 1968).

<sup>14</sup>G. F. Bertsch, *Phys. Rev. Lett.* **34**, 697 (1975).

<sup>15</sup>D. E. Greiner, P. J. Lindstrom, H. H. Heckman, B. Cork, and F. S. Bieser, *Phys. Rev. Lett.* **35**, 152

(1975); P. J. Lindstrom, D. E. Greiner, H. H. Heckman, B. Cork, and F. S. Bieser, LBL Report No. LBL-3650, 1975 (unpublished); H. H. Heckman and P. J. Lindstrom, *Phys. Rev. Lett.* **37**, 56 (1976).

<sup>16</sup>It should be noted that *viscous* hydrodynamics assumes small deviations from local thermal equilibrium and thus also  $\Lambda \ll R$ . Although it can give a qualitative description of shock structure it is not adequate for conditions such as a shock which involve large deviations from equilibrium.

<sup>17</sup>A. R. Bodmer and C. N. Panos, *Bull. Am. Phys. Soc.* **21**, 13 (1976); in *Proceedings of the Symposium on Macroscopic Features of Heavy-Ion Collisions* [Argonne National Laboratory, Report No. ANL-PHY-76-2, May, 1976 (unpublished)], p. 463.

<sup>18</sup>Classical microscopic (Newtonian) calculations have also been made by A. D. MacKellar, L. Wilets, and G. A. Rinker, Jr., *Bull. Am. Phys. Soc.* **21**, 13 (1976); in *Proceedings of the Symposium on Macroscopic Features of Heavy-Ion Collisions* (see Ref. 17), p. 663; relativistic considerations are also presented in *Fourth International Workshop on Gross Properties of Nuclei and Nuclear Excitations*, Hirschegg, Austria, 1976 (unpublished).

<sup>19</sup>Classical microscopic calculations which use a more probabilistic approach and are closely related to cascade-type calculations have been made by J. P. Bondorf, H. Feldmeier, S. Garpman, E. C. Halpert and P. J. Siemens, in *Proceedings of the Symposium on Macroscopic Features of Heavy-Ion Collisions* (see Ref. 17), p. 601; *Classical Microscopic Calculation of Fast Heavy-Ion Collisions*, The Niels Bohr Institute, Copenhagen, Report, 1976 (unpublished).

<sup>20</sup>For nucleon-nucleus cascade calculations, see: N. Metropolis, R. Bivins, M. Storm, A. Turkevich, J. M. Miller, and G. Friedlander, *Phys. Rev.* **110**, 185 (1958); **110**, 204 (1958); H. W. Bertini, *ibid.* **131**, 1801 (1963); K. Chen, Z. Fraenkel, G. Friedlander, J. R. Grover, J. M. Miller, and Y. Shimamoto, *ibid.* **166**, 949 (1968). R. K. Smith and M. Danos (private communication) are making relativistic heavy-ion cascade calculations in the GeV/nucleon range.

<sup>21</sup>We use a predictor/corrector algorithm of C. W. Gear [ANL Report No. ANL-7126, 1966 (unpublished)].

Typical computing times (IBM 360/195) for 1000 steps are 70, 250, and 500 s for  $A=100, 250,$  and  $400,$  respectively.

<sup>22</sup>Approximate treatments involving linearizations of the Boltzmann equation or the assumption of unchanged target and projectile distributions in cascade calculations, cannot describe the more equilibrated central collisions in which the final distributions are very different from the initial ones. Approximate treatments based on the use of "undepleted" initial distributions are closely related to Glauber-approximation treatments of the peripheral collisions, as discussed by J. Hüfner, K. Schäfer, and B. Schürmann, *Phys. Rev. C* **12**, 1888 (1975); A. Abul-Magd, J. Hüfner, and B. Schürmann, *Phys. Lett.* **60B**, 327 (1976).

<sup>23</sup>Ideal-gas hydrodynamics corresponds to the double limit  $L \gg \Lambda \gg d(\tau_{NN} \ll \tau_{rel} \ll \tau_{col})$ , where  $L \gg \Lambda$  is required for local thermodynamic equilibrium. Note that hydrodynamics only assumes  $\Lambda \ll L$  and is, in general, not obtainable via the Boltzmann equation.

<sup>24</sup>Modifications and extensions of inviscid hydrodynamics are the use of viscous hydrodynamics by J. A. Maruhn, T. A. Welton, and C. Y. Wong—Physics Division Annual Progress Report [Oak Ridge National Laboratory Report No. ORNL-5137, May 1976 (unpublished)], p. 134—who have made one-dimensional calculations for the collision of two slabs, and the use of a two-fluid description. The latter assumes separate fluids for the projectile and target nuclei and thus allows for the persistence of projectile and target due to transparency effects. Such two-fluid calculations are being made by A. A. Amsden, A. S. Goldhaber, F. H. Harlow, and J. R. Nix.

<sup>25</sup>A good example of this twofold role is the work of V. Ruck, M. Gyulassy, and W. Greiner, *Z. Phys.* **A277**, 391 (1976) on pion condensation in heavy-ion collisions. Thus, as they emphasize, the role of a pion condensate in heavy-ion collisions may be not so much through its effect on the equation of state, but rather in reducing  $\Lambda$  and thus "triggering" hydrodynamic conditions. This is envisaged to occur through the critical fluctuations associated with the onset of the condensate, these fluctuations enhancing the  $N-N$  cross sections above their free-space values.

<sup>26</sup>Currently we are using a somewhat more elaborate procedure (involving an extra stage and the use of a single-particle containing potential) which, however, gives much the same results.

<sup>27</sup>We have also considered a device which tests and partially obviates changes due to self-interactions of each nucleus during the early stages of the collision. This device consists essentially in letting only those nucleons interact which are within a sphere whose radius is conservatively taken as  $v \cdot t + d$  where  $d \approx 3$  fm and  $v$  is the laboratory velocity. The remaining nucleons are transported with the initial c.m. velocity of their nucleus and with their initial velocities unchanged. This device is clearly only operative during the early stages of the collision and energy is then only approximately conserved. It is satisfactory that the results with and without this device are quite similar.

<sup>28</sup>We have also made less complete calculations for  $A_1 = 50, A_2 = 200,$  and for  $A_1 = A_2 = 200.$

<sup>29</sup>Our analysis programs average around the incident

direction. Because of the symmetry around this direction, this average is equivalent to averaging the initial conditions (for a given  $b$ ) around the incident direction as is appropriate to the physical situation.

<sup>30</sup>H. A. Bethe and M. B. Johnson, *Nucl. Phys.* **A230**, 1 (1974).

<sup>31</sup>See, e.g., N. F. Mott and H. S. W. Massey, *The Theory of Atomic Collisions* (Oxford U.P., 1965), pp. 631–634; S. Chapman and T. G. Cowling, *The Mathematical Theory of Non-Uniform Gases*, (Cambridge, U.P., 1970) 3rd ed.; J. O. Hirschfelder, C. F. Curtiss, and R. B. Bird, *Molecular Theory of Gases and Liquids* (Wiley, New York, 1954).

<sup>32</sup>For the  $np$  differential cross sections we used very convenient fitting expressions obtained in the energy range between 22.5 and 400 MeV by A. Rindi, C. B. Lim, and T. Salmon-Cinotti, Lawrence Radiation Laboratory Report No. UCRL-20295, November 1970 (unpublished). For the  $pp$  cross sections we used scattering data from a number of sources referenced in R. A. Arndt, R. H. Hackman, and L. D. Roper, *Phys. Rev. C* **9**, 555 (1974).

<sup>33</sup>Thus, e.g., for "nucleus" 1, i.e., for nucleons  $i=1, \dots, A_1,$  one has  $T(t) = \frac{1}{2} M [\sum_{i=1}^{A_1} \vec{v}_i(t)/A_1]^2$ , where  $M$  is the nucleon mass. For  $A_1=A_2$  the value of  $T(t)$  is the same for both "nuclei."

<sup>34</sup>Because the correction is fairly small, correction by subtraction, e.g.,  $W_f = W(t_f) - \delta W$  where  $\delta W = W_{NI}(t_f) - W_i \approx 4$  MeV, gives almost the same results as correction by scaling.

<sup>35</sup>Thus if, for a central collision with  $b=0,$  the initial internal kinetic energy were zero and if also the c.m. angular distribution were isotropic and the final nucleons all had the same kinetic energy, then the final c.m. velocities would all have the same magnitude of  $0.5v.$

<sup>36</sup>Thus A. S. Goldhaber (private communication) has suggested that information about the impact parameter may be obtainable from correlations (coincidences) between nucleons observed in the projectile and target frames of reference.

<sup>37</sup>The continuation of this trend (of increasing transparency) to higher energies ( $\geq$  GeV/nucleon) would imply that the cross section for "violent" well-equilibrated central collisions would then become much reduced (or even zero) and that shock-type phenomena should be much less prominent, or not occur at all, at these energies (see the discussion in Ref. 6). This seems inconsistent with the available evidence (Refs. 15, 38, and 40).

<sup>38</sup>M. Buenerd, C. K. Gelbke, B. G. Harvey, D. L. Hendrie, J. Mahoney, A. Menchaca-Rocha, C. Olmer, and D. K. Scott, *Phys. Rev. Lett.* **37**, 1191 (1976).

<sup>39</sup>See, e.g., L. G. Moretto, in Proceedings of the Symposium on Macroscopic Features of Heavy-Ion Collisions (see Ref. 17), p. 235.

<sup>40</sup>H. H. Gutbrod, A. Sandoval, P. J. Johansen, A. M. Poskanzer, J. Gosset, W. G. Meyer, G. D. Westfall, and R. Stock, *Phys. Rev. Lett.* **37**, 667 (1976).

<sup>41</sup>A. D. MacKellar and L. Wilets (Ref. 18) have suggested a procedure for "relativizing" a static potential which assumes neglect of accelerations.

<sup>42</sup>This is being done in collaboration with A. D. MacKellar.

<sup>43</sup>See, e.g., J. Stachel and P. Havas, *Phys. Rev. D* **13**,

1598 (1976), and references cited there, for Hamiltonian and Lagrangian formulations which are Lorentz invariant to order  $c^{-2}$  and which involve only particles interacting directly through potentials.

<sup>44</sup>See, e.g., H. W. Bertini, *Phys. Rev.* 188, 1711 (1969); *Phys. Rev. C* 6, 631 (1972); G. D. Harp, K. Chen, G. Friedlander, Z. Fraenkel, and J. M. Miller, *ibid.* 8, 581 (1973); G. D. Harp, *ibid.* 10, 2387 (1974).

<sup>45</sup>L. Wilets (private communication) has proposed a momentum-dependent potential which is designed to simulate the effect of the Pauli principle and at the

same time to give adequate saturation and scattering properties. We are also looking at more purely phenomenological momentum-dependent potentials.

<sup>46</sup>A critical problem is the numerical evaluation of gradient terms, e.g.,  $\vec{\nabla}\rho$ , by suitable averaging over the particle positions.

<sup>47</sup>This term, which corresponds to the average force term in the Vlasov equation, has the form  $-(\vec{F}(\vec{x};t)/m) \cdot \vec{\nabla}_v f(\vec{x}, \vec{v}; t)$ , where  $f$  is the distribution function and  $\vec{F}$  is the average force.